Jiang *et al. Chin. J. Mech. Eng.* (2019) 32:94
https://doi.org/10.1186/s10033-019-0408-9

Chinese Journal of Mechanical Engineering

ORIGINAL ARTICLE Open Access

Optimization of Cutting Parameters for Trade-off Among Carbon Emissions, Surface Roughness, and Processing Time

Zhipeng Jiang[1], Dong Gao[1], Yong Lu[1*] and Xianli Liu[2]

Abstract

As the manufacturing industry is facing increasingly serious environmental problems, because of which carbon tax policies are being implemented, choosing the optimum cutting parameters during the machining process is crucial for automobile panel dies in order to achieve synergistic minimization of the environment impact, product quality, and processing efficiency. This paper presents a processing task-based evaluation method to optimize the cutting parameters, considering the trade-off among carbon emissions, surface roughness, and processing time. Three objective models and their relationships with the cutting parameters were obtained through input–output, response surface, and theoretical analyses, respectively. Examples of cylindrical turning were applied to achieve a central composite design (CCD), and relative validation experiments were applied to evaluate the proposed method. The experiments were conducted on the CAK50135di lathe cutting of AISI 1045 steel, and NSGA-II was used to obtain the Pareto fronts of the three objectives. Based on the TOPSIS method, the Pareto solution set was ranked to find the optimal solution to evaluate and select the optimal cutting parameters. An S/N ratio analysis and contour plots were applied to analyze the influence of each decision variable on the optimization objective. Finally, the changing rules of a single factor for each objective were analyzed. The results demonstrate that the proposed method is effective in finding the trade-off among the three objectives and obtaining reasonable application ranges of the cutting parameters from Pareto fronts.

Keywords: Automobile panel dies, Carbon emission, Parameter optimization, Multi-objective optimization, NSGA-II

1 Introduction

In 2017, the total number of automobiles in China reached 217 million, and has shown an increasing trend each year [1]. In recent years, the upgrading of cars has accelerated which has caused an acceleration of the need for automobile panel dies. The design and manufacturing times of automobile panel dies accounts for 2/3 of the automobile development cycle [2], and therefore the processing efficiency and quality of the die directly restrict the speed of an auto body modification. There are large numbers of rotating machinery parts on the die. Turning is a necessary process for the machining of rotary parts, such as ejector pins [3]. However, carmakers have been striving to maximize profits, putting their economic benefit first and ignoring the environmental attributes of their products. Carbon emissions (C) are the major causes of global problems, such as the melting of the Arctic and Antarctic glaciers, rising sea levels, and global warming. To neutralize or alleviate the environmental pressure of carbon emissions, and to achieve the sustainable development of the economy, society, and future generations, countries around the world have jointly formulated a series of environmental laws and regulations and related standards. The international community first enacted an environmental-related law (United Nations Framework Convention on Climate Change) in 1992 to meet the challenge of global warming. The enforcement of the Kyoto Protocol in 2005 marked the entry into a

*Correspondence: luyong@hit.edu.cn
[1] School of Mechatronics Engineering, Harbin Institute of Technology, Harbin 150001, China
Full list of author information is available at the end of the article

substantial phase of reducing greenhouse gases in the international community [4].

Lightweight design technologies used in machine tool structures, 3-R manufacturing, the application of new processing technologies and other aspects are potential measures for energy saving and a reduction of emissions in the manufacturing industry [5]. However, these measures are difficult to apply widely within a short time.

There is a massive amount of existing machine tools in reserve, and parameter optimization for existing machine tools and processing technology is not only an effective way to improve the processing quality and efficiency [6], it is also an effective measure in energy saving and the reduction of emissions [7]. Therefore, parameter optimization has become a hotspot in current research. Campatelli et al. [8] employed an experimental approach to model the energy consumption in the milling of AISI 1050 carbon steel, and claimed that increasing the material removal rate (MRR) as much as possible will help reduce energy consumption during the processing. Wójcicki et al. [9] adopted a model-based approach for a systematic energy efficiency evaluation and optimization during turning operations, combining a spindle, chiller, and material removal models, and taking into account the strong interrelations between the cutting process, a spindle with a permanent magnet motor, and its chiller. Zhong et al. [10] considered the effects of the cutting parameter combinations on the energy consumption at a certain material removal rate, and based on this discovery, considered a specific energy consumption as the optimization goal and took the cutting parameters as the optimization variables during the material removal process during the turning; cutting parameter sets with a large feed rate were then recommended. Bilga et al. [11] regarded the cutting speed, feed rate, cutting depth, and nose radius along with their interactions as the variables to optimize energy consumption, and showed that the feed rate is the vital dominating parameter for a reduction of the energy consumed; however, the nose radius does not contribute much. To lower the specific cutting energy in high-speed milling, Wang et al. [12] took 7050-T7451 aluminum alloy as the processing object to reveal the influence of the cutting speed, undeformed chip thickness, and tool rake angle on the cutting energy consumption.

However, parameter optimization aiming at minimizing the environmental cost (energy consumption or carbon emission) often sacrifices the economy of the mechanical products, machining processes, or product performance. Therefore, parameter optimization constrained by multiple optimization objectives has received increasing attention. Wang et al. [13] took energy consumption, cost, and surface roughness as the optimization objectives, and applied NSGA-II as a tool for multi-objective parameter optimization. The results show that the parameter optimization has a significant energy saving effect, but shows little improvement of the surface roughness. Based on the proposed system boundary of energy consumption, Yi et al. [14] took the surface roughness as a constraint along with the cutting speed and feed rate to further optimize the carbon emissions and processing time simultaneously. Liu et al. [15] took the cost of carbon emissions into account, taking the cutting speed and feed rate as decision variables, and carbon emissions and the processing time as the optimization objectives to analyze the relationship between decision variables and the optimization objectives. He et al. [16] proposed the establishment of a multi-objective optimization model that takes the cutting parameters as the decision variables, and the energy consumption, cutting force, and time as the performance indicators for the turning and milling processes. Non-inferior optimal target areas were obtained through a theoretical analysis, experimental design, and statistical regression. Bagaber et al. [17] took the dry cutting of stainless steel 316 with high strength and corrosion resistance as an example and carried out an orthogonal experiment with three factors and five levels using an uncoated cemented carbide tool. Good results were achieved on reducing the energy consumption, improving the surface quality, and prolonging the tool life. Lin et al. [18] proposed a multi-objective teaching–learning-based optimization algorithm during an entire turning operation, which is intended to minimize the carbon emissions and operation time simultaneously by optimizing the cutting parameters; later, the analytic hierarchy process was used to find the optimal solution among the available Pareto-optimal solutions. Camposeco-Negrete [19] presented an experimental study to optimize the cutting parameters in the rough turning of AISI 6061 T6 aluminum and establish the restrictive relationship among the energy consumption, surface roughness, and MRR; meanwhile, it was pointed out that the feed rate and cutting depth are significant factors for minimizing the specific energy consumption, although to minimize the surface roughness, the feed rate was determined to be the most significant factor. Lin et al. [20] used a teaching–learning-based optimization algorithm to deal with the relationships between carbon emissions, operation time, machining time, and cutting parameters for both dry and wet turning environments, and the research results show that the use of cutting fluids has a vital catalytic role in reducing the carbon emissions and processing times and improving the production efficiency. Tansel [21] considered existing research on the trade-offs among directly related environmental, economic, and quality objectives to be either incomplete or inaccurate, and used three analysis methods (the RSM-based Goal Programming model, TOPSIS-based Taguchi approach, and Grey Relational Analysis-based Taguchi approach) to analyze the coupling relationship between cutting parameters and different tools (multi-coated TiCN+Al2O3+TiN, surface carbon coating, and diamond coating), and different materials (6061, 6082, and 7075). The results show that the RSM-based Goal Programming approach is generally better than the other two. Li et al. [22] used a multi-objective particle swarm optimization algorithm as a tool to minimize the energy and processing time simultaneously through the optimization of the cutting parameters during CNC milling, and pointed out that the width of cut is a major process parameter affecting both the energy and processing time. To address the problem of a simultaneous optimization of the cutting parameters and processes, Zhang et al. [23] used an improved universal gravity search algorithm to establish a two-part search space for the cutting parameters and process layout, and proposed a target optimization model for minimizing the processing time and carbon emissions.

A comparison of the literature on the optimization of environmental indicators in recently published studies is shown in Table 1. Summarizing the findings of the thorough literature review above, it can be claimed that the current studies on parametric optimization for minimizing the negative environmental influence present the following shortages.

1. Numerous parameter optimization models only take energy consumption, carbon emissions, or other environmental indicators as the optimization objective, which often sacrifice processing efficiency or product quality, and are extremely one-sided. To fully analyze the trade-offs among environmental, product quality, and efficiency indicators, for example, minimizing the carbon emissions and processing time and maximizing the product quality, multi-objective parameter optimization is worth studying.
2. The optimal parameters in many studies are directly derived from experimental parameter combinations, the results of which are extremely dependent on the selected experimental parameters. If the experimental parameters are not chosen well, they are easily trapped into the local optimum.
3. In multi-objective optimization studies using carbon emissions as an indicator, the same cutting depth is often specified, or the carbon emissions are calculated after a single cutting according to the orthogonal test table. Although the former applies the same processing tasks, it limits the cutting depth and the parameter optimization is not comprehensive. The latter will result in a different amount of material removed owing to a different cutting depth, and the results lack comparability.

As shown in Table 1, energy consumption minimization is usually selected as an environmental indicator in the literature. However, compared with energy consumption, carbon emissions can more fully reflect the environmental impact of the machining process, and are more in line with the actual situation. Surface roughness is one of the commonly used indicators for evaluating the product quality. Different surface roughness thresholds may cause large changes in the processing time, tool wear, carbon emissions, and other factors. The surface roughness is a reasonable indicator of the surface quality. The processing time largely determines the market competitiveness of the products and the ability to cope with market risks. It is also an important indicator used to measure the technical and management level of an enterprise. It is therefore reasonable to take lower carbon emissions, a lower surface roughness, and a lower processing time as the optimization objectives. In terms of the decision variable selection, cutting parameters directly affect the carbon emissions, surface quality, and processing time, and thus the cutting parameters were chosen as the decision variables. During actual processing, the workpiece material is often selected long in advance, and there is no need to apply an optimization. Cutting tools have an effect on the optimized targets and a particular optimization space [24], which can be used as one of the decision variables. However, in an investigation into the factory setting, it was found that the tool used is relatively fixed and that the tool parameters cannot be easily replaced. For the time being, however, this is not considered as a control variable in the present study.

This study aims to achieve high efficiency, high precision, and low environmental costs for sustainable machining by optimizing the cutting parameters without replacing the machine tools or other equipments. The optimization method simplifies the parameter optimization when considering multiple factors, allowing it to become easily popularized. In this way, sustainable processing can be realized without increasing the production cost of an enterprise, and products with a better green performance can be produced, which is helpful to enhance the market competitiveness of the enterprise. Therefore, NSGA-II and TOPSIS were taken as algorithm tools, the processing task was used as the evaluation objective, the cutting parameters were applied as decision variables, and the carbon emissions, surface roughness, and processing time were used as the optimization objectives to study the balance

Table 1 Comparison among the proposed optimization algorithm and other studies in the literature

	Process	Control variable					Performance criteria					
		Cutting speed	Feed rate	Cutting depth	Width of cut	Others	Environmental indicator		Processing time	Cost	Surface roughness	Others
							Energy consumption	Carbon emission				
Campatelli et al. (2014) [8]	Milling	√	√	√	√		√					
Wójcicki et al. (2018) [9]	Turning	√	√	√			√					
Zhong et al. (2017) [10]	Turning	√	√	√			√					
Bilga et al. (2016) [11]	Turning	√	√	√			√					
Ma et al. (2017) [24]	Milling	√	√			Cutting fluid flow rate	√					Cutting fluid
Lin et al. (2015) [18]	Turning	√	√	√				√	√			
Li et al. (2016) [22]	Milling	√	√	√	√		√		√			
Wang et al. (2014) [13]	Turning	√	√	√			√			√	√	
Li et al. (2013) [25]	Turning	√	√	√				√	√			
Yi et al. (2015) [14]	Turning	√	√					√	√			
Camposeco-Negrete (2015) [19]	Turning	√	√	√			√				√	
Liu (2016) [15]		√	√					√	√			
He et al. (2017) [16]	Turning/milling	√	√	√	√		√		√			Cutting force
Salem Abdullah Bagaber (2017) [17]	Turning	√	√	√			√				√	Tool wear
Zhang et al. (2017) [23]	Turning/milling	√	√			Scheduling	√		√			
Lin et al. (2017) [20]	Turning	√	√	√				√	√	√		
Yusuf Tansel (2018) [21]	Turning	√	√	√		Cutting tool and workpiece material		√			√	
The improved study	Turning	√	√	√				√	√		√	

between each objective and achieve a better surface quality, shorter processing time, and less environmental costs.

2 Methods

Facing increasingly severe environmental problems, the trade-off and restrictive relationship among the processing efficiency, processing quality, and environmental impact were studied along with the optimization of the cutting parameters as decision variables to reduce the environmental impact, and improve the processing quality and efficiency. First, existing optimization models of the cutting parameters when considering the environmental impact were analyzed, and it was found that the multi-objective optimization model is a popular but difficult research topic. In view of the existing problems of this research, carbon emissions, the processing time, and the surface roughness were selected in this study as the optimization objectives, with the cutting parameters as the decision variables; RSM, NSGA-II, and TOPSIS as the technical means; and the processing task as the research object used to solve the multi-objective optimization problem. Figure 1 shows the organization of the present paper.

First, three objective models and their relationships with the cutting parameters are needed, namely, the modeling carbon emissions model based on an input–output analysis to ensure the reliability of the system boundary, a response surface analysis to model the surface roughness to ensure the accuracy of the prediction, and a mathematical method to build the processing time model to ensure the accuracy of the processing time calculation. The mathematical relationships used to establish the processing task-based multi-objective optimization model for high-efficiency, low carbon emissions, and high-quality processing manufacturing are described in Section 3.

A turning case study is given in Section 4, and the multi-objective optimization equation is derived according to the experiment results.

The results and a discussion of the optimal Pareto solutions are presented in Section 5. NSGA-II was selected as the multi-objective optimization method to obtain the Pareto frontier. The optimal solution was obtained by sorting the Pareto solution set based on TOPSIS. A main effect analysis was carried out to find the ranking of significant factors. Contour maps were drawn through a simulation analysis to analyze the interaction between the decision variables and optimization objectives. Subsequently, a sensitivity analysis was carried out to analyze and explain the changing rules between the objectives and decision variables.

Finally, some concluding remarks are given.

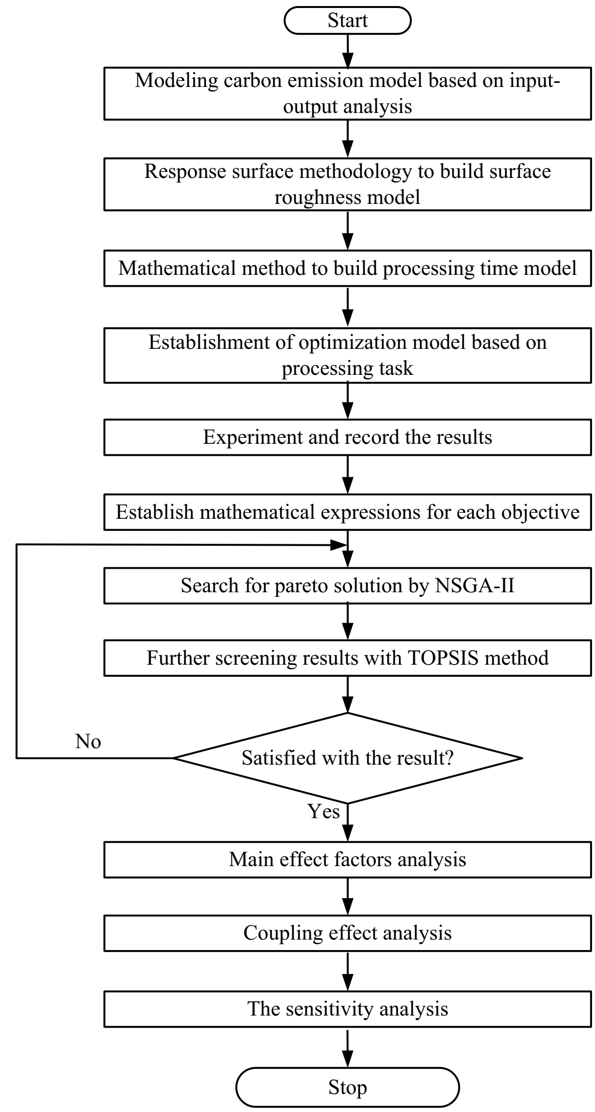

Figure 1 Flow chart of the present paper

3 Multi-Objective Optimization Model

3.1 Decision Variables

In this study, the traditional turning process was selected as the research object for multi-objective optimization research, although the research method and theory can be applied to other machining processes. As mentioned in Section 1, the spindle speed, cutting depth, and feed rate were selected as decision variables.

3.2 Targets to be Optimized

3.2.1 Carbon Emission

An input–output analysis was originally applied to the field of economics, and the concept was quickly applied to other areas, playing an important role in describing the relationship between the final demand and total outputs from an up-down perspective. The carbon emission model of the machine tools used during the cutting process should not only consider the carbon emissions produced by electric energy consumption, but also the carbon emissions produced by auxiliary equipment, tools, and cutting fluid. An input–output analysis is used to analyze the carbon emissions during the machining processes to ensure the accuracy of the carbon emission calculation, as shown in Figure 2. The machining process requires the input of power and resources, in addition to the target products, and is also accompanied by a large amount of waste generated at the output. According to the consumption form of the energy resources used during the machining process, carbon emissions are divided into consumable and transferable carbon emissions. Consumable carbon emissions refer to carbon emissions from the electricity consumed during the machining process. The use of electricity does not produce carbon emissions, but the production process of electricity does. Carbon emissions from electric power are obtained by multiplying the electricity consumption by the electricity carbon emission factor (Eq. (2)). A calculation of the electricity consumption of CNC machine tools can be found in a previous study [26]. Transferable carbon emissions refer to the carbon emissions transferred from raw materials, cutting tools, cutting fluids, and other resources during the processing, which are transformed into waste materials such as chips, scrap cutting tools, and scrap cutting fluids. That is, transferable carbon emissions include two parts: input resource carbon emissions and output waste carbon emissions. As the calculation method, the mass/volume is multiplied by the carbon emission coefficient. Products are effectively exported, regardless of the carbon emissions produced. Because a processing task-based optimization model is adopted in this paper, the amount of material removed is also fixed, which cannot and does not need to be optimized. Therefore, this part of the carbon emissions is not calculated in this multi-objective optimization

$$C = C_{consum} + C_{trans}, \tag{1}$$

$$C_{consum} = CF_{ene} \times E_{ene}, \tag{2}$$

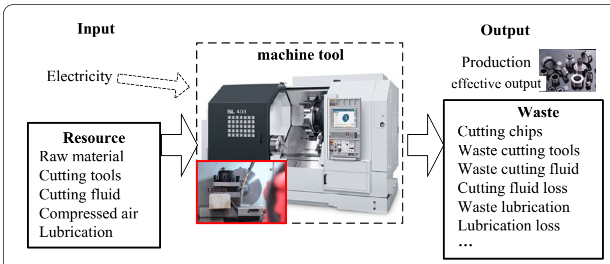

Figure 2 Input–output analysis of machine tools

$$C_{trans} = C_{resource} + C_{waste}, \tag{3}$$

$$C_{resource} = C_{tool} + C_{cool} + C_{air}, \tag{4}$$

$$C_{waste} = C_{chips} + C_{tool-w} + C_{cool-w}, \tag{5}$$

3.2.2 Surface Roughness

The formation of the surface roughness during the mechanical cutting process can be roughly summarized into three factors: geometric factors, physical factors, and vibrations of the process system. Geometric factors refer to the residual area of the cutting layer left behind on the machined surface when the tool moves relative to the workpiece. Many theoretical surface-quality calculation models are calculated based on this characteristic [27]. The actual surface roughness after cutting has a large difference from the theoretical roughness, which is mainly affected by the physical properties of the material being processed and the cutting mechanism. During the cutting process, the edge fillet of the tool and the flank surface will be plastically deformed by pressing and rubbing against the workpiece. The higher the toughness, the greater the plastic deformation of the material, allowing built-up edge and scale to easily appear, seriously deteriorating the roughness. The vibration of the processing system, such as the cutting parameters and the cooling lubricants, is an important factor affecting the surface roughness, and is an important means to control and improve the surface roughness during actual cutting. In this paper, the quality of dry turning is improved by changing the cutting parameters. For dry turning, in this study, the machining quality is improved by changing the cutting parameters. Because the surface roughness of the workpiece is a non-linear process, a second-order polynomial response surface mathematical equation is utilized, as shown in Eq. (6), and the coefficients of the function can be obtained using the least squares method.

$$R_a = \beta_0 + \sum_i \beta_i h_i + \sum_{i<j} \beta_{ij} h_i h_j + \sum_i \beta_{ii} h_i^2 + \varepsilon, \tag{6}$$

where h represents the turning parameters (spindle speed, feed rate, and depth of cut), β is the coefficient of each term, and ε is a residual error.

3.2.3 Processing Time

Taking machine tools as a whole as the research object, the machining processing time T_{machin} refers to the time required to complete the processing of a part, which consists of the maneuver time (also known as the basic time) $t_{maneuver}$ and auxiliary time $t_{auxiliary}$.

$$T_{machin} = t_{auxiliary} + t_{maneuver}. \tag{7}$$

The maneuver time $t_{maneuver}$ is the cutting time needed to directly change the size, shape, and surface quality of the workpiece, including the stand-by time and idle running time.

$$t_{maneuver} = t_{stand-by} + t_{idle} + t_{cut}. \tag{8}$$

The idle running time, t_{idle}, is determined as indicated in Figure 3.

$$\begin{aligned} t_{idle} = {} & \max\left(\frac{L_{x1}}{v_{fx}}, \frac{L_{z1}}{v_{fz}}\right) + \sum_{j=1}^{N}\left[\frac{L_{z2j}}{v_f} + \frac{L_{x2j}}{v_f} + \frac{L_{z3j}+L_{z2j}}{v_{fz}} + \frac{L_{x2j}}{v_{fx}}\right] \\ & + \max\left(\frac{L_{x1}-L_{x2}}{v_{fx}}, \frac{L_{z1}+L_{z2}+L_{z3}}{v_{fz}}\right), N = 1,2,3,\cdots \\ L_{x2j} = {} & L_{x2} + j \cdot a_p. \end{aligned} \tag{9}$$

$$t_{cut} = \sum_{j=1}^{N}\left[\frac{L_{z3j}}{v_f}\right], N = 1,2,3,\cdots \tag{10}$$

The auxiliary time $t_{auxiliary}$ is the time consumed by various auxiliary actions used to process each workpiece during a certain process, such as starting and stopping the machine tools, changing a tool, trial cutting, measurements, and other related steps consuming auxiliary action time. In this study, AISI 1045 steel was processed, and the processing task was small. It is considered that the auxiliary times of each group of processing tasks are the same, and thus there is no room for optimization, which can be omitted for convenience, and that the stand-by time is the same.

$$t_{auxiliary} = t_{clam} + t_{set} + t_{pro} + \frac{t_{chan} \cdot t_{cut}}{T_{tool}} + t_{unl}. \tag{11}$$

According to the generalized Taylor formula [28], the tool life is as shown in Eq. (12):

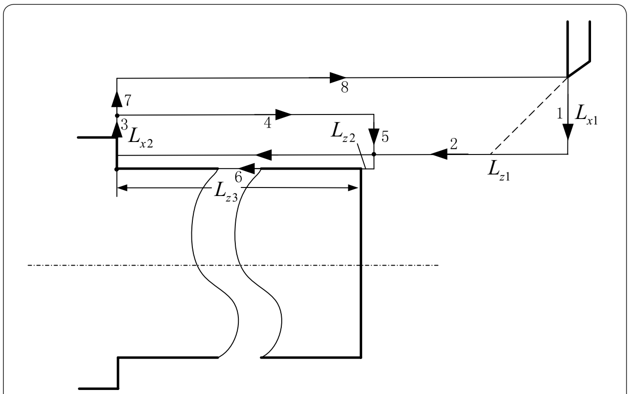

Figure 3 Turning path diagram

$$T_{tool} = \frac{A^{1/m}}{v_c^m \cdot a_p^{x/m} \cdot f^{y/m}}. \tag{12}$$

3.3 Constrains

For the diversity of the materials to be processed, the processing equipment, and fine and rough processing technology, the proper values of the cutting parameters will be within a different interval. At the same time, the range of the cutting parameters will be defined by the processors based on personal experience. Therefore, for the specific practical machining process, the cutting parameters should be restricted to a certain scope to avoid unnecessary calculations and a waste of resources.

Combined with the above research, a multi-objective optimization equation is obtained.

$$\min\{C, t, Ra\}, \tag{13}$$

$$\text{s.t.,} \begin{cases} n_{\min} \le n \le n_{\max}, \\ f_{\min} \le f \le f_{\max}, \\ a_{p-\min} \le a_p \le a_{p-\max}. \end{cases} \tag{14}$$

4 Case Study

4.1 Experiments and Data Acquisition

The turning process was taken as the research object. The experimental scenarios were carried out on a SMTCL CAK50135di CNC lathe with a spindle power of 6.5 kW, and its maximum spindle speed can reach 1450 r/min. The fast forward speed of the machine tool is 1900 mm/min. A carbide cutting tool was employed for the experiment. The cutting tool material is YT15 and the rake angle is 10°, the main cutting-edge angle is 75°, and the tool tip radius is 1 mm. Some AISI 1045 steel bars with dimensions of $\phi 90 \times 120$ mm were employed. The hardness of the steel is 187 HB, and its composition is 0.42%–0.50%C, 0.50%–0.80%Mn, 0.17%–0.37%Si, and ≤0.25%Cr [29].

The experimental setup is shown in Figure 4. The power requirement during the mechanical machining process was measured using a WT333 type digital power meter (Yokogawa). The measurement software provided by the manufacturer is WTViewerFreePlus. This type of measurement equipment can be used to measure all AC and DC parameters; moreover, integral and harmonic measurements can be conducted at the same time without changing the measurement mode. The limits of the measured current can be as low as 50 μA and as high as 40 A. The sampling frequency is 10 Hz, and the reading accuracy is 0.1%. For a more detailed description of the experiment, refer to our previous study [26]. A surface roughness measurement was conducted using a Tr200V1.5 surface roughness meter (Beijing Times Rui Da Technology Co., Ltd.) with a range of 0.005–80 μm.

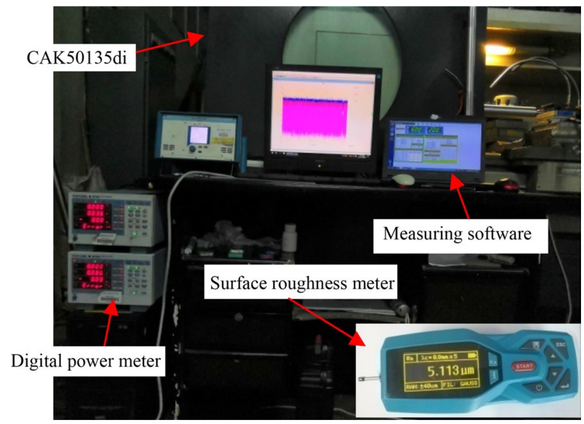

Figure 4 Experiment setup

To establish a regression model of the surface roughness, a bar with a diameter of 66.5 mm was selected as the test object according to the actual experiment conditions. The central composite design can fit the response surface better than the Box–Benhnken design. At the same time, it is advisable that the experiment level not exceed the boundary of the cube to avoid exceeding the processing capacity of the machine. To reduce the number of experiments and ensure the accuracy of the results, the central composite inscribed design method was selected. The value of α was set to ±1. Table 2 shows the experiment design and results.

As mentioned above, to ensure the comprehensiveness of the parameter optimization and the comparability of the results, a task-based parameter optimization method was chosen. The designated processing task is to process a bar with a diameter of 90–84 mm, the cutting length is equal to 30 mm. In addition, it is assumed that the machine starts to perform a fast forward after 30 s of a standby period.

To establish a multi-objective optimization equation, the following parameters or data need to be measured and acquired.

According to the actual measurement of SMTCL CAK50135di, the stand-by power under the selected cutting parameter is 321 W. The tool used is produced by Zhuzhou Cemented Carbide Cutting Tools Co., Ltd. The cutting tool material is YT15 and its weight is 474 g.

The cutting fluid needs regular supplementation and replacement, and according to an investigation on machine tools, the coolant is water-based, the specifications of the cutting fluid is 20 L/barrel, the ratio of oil to water is 1:10, and the frequency of replacement is 5 months. The machine tool runs 22 days per month, with coolant applied for 8 h per day. The remaining coolant to be replaced is approximately 8 L.

Table 2 Design of regression analysis experiment

	n (r/min)	f (mm/r)	a_p (mm)	R_a (μm)
1	600	0.1	0.30	5.113
2	450	0.2	2.00	14.700
3	600	0.3	2.00	18.538
4	300	0.2	1.15	15.620
5	300	0.1	0.30	5.373
6	300	0.3	0.30	18.349
7	300	0.1	2.00	5.209
8	450	0.2	1.15	15.916
9	450	0.3	1.15	17.919
10	600	0.2	1.15	14.727
11	600	0.3	0.30	17.985
12	450	0.2	1.15	15.812
13	450	0.2	1.15	15.462
14	600	0.1	2.00	4.907
15	450	0.2	1.15	15.976
16	450	0.2	1.15	15.113
17	450	0.1	1.15	6.028
18	450	0.2	0.30	14.977
19	450	0.2	1.15	15.090
20	300	0.3	2.00	19.630

Table 3 Equivalent carbon emission factors

Name of carbon emission factors	Quantitative value
CF_{ene} (g-CO_2/kW·h)	724.2
CF_{tool} (g-CO_2/kg)	29600
CF_{c_pro} (g-CO_2/L)	2850
CF_{c_dis} (g-CO_2/L)	4000
$CF_{material}$ (g-CO_2/kg)	2690
$CF_{disposal}$ (g-CO_2/kg)	361

The carbon emission factors used are as shown in Table 3.

4.2 Establishment of Multi-Objective Optimization Model

The experiment data recorded in Table 2 can be regressed using a response surface method, see Appendix A for details, and the surface roughness model is therefore as follows:

$$R_a = -11.556 + 203.16f - 343.4f^2. \tag{15}$$

Applying the above data, combined with Section 3, the multi-objective optimization equations for machining tasks is obtained, and at the same time, the restrictive conditions are given according to the actual situation.

$$\min\begin{cases} C = 724.2 \times E_{ene} + \frac{t_{cut}}{T_{tool}} \times CF_{tool} \times M_{tool} + \frac{(t_{cut}+t_{idle})}{3168} \times 89, \\ t = t_{cut} + t_{idle}, \\ R_a = -11.556 + 203.16f - 343.4f^2, \end{cases} \tag{16}$$

$$\text{s.t.,}\begin{cases} 300 \le n \le 600, \\ 0.1 \le f \le 0.3, \\ 0.3 \le a_p \le 2, \end{cases} \tag{17}$$

where

$$\begin{aligned} E_{ene} = &\frac{\left[321.4 \times 30 + \left(750.9 + 115.4 \times n/60 + 11.32 \times (n/60)^2\right) \times t_{idle}\right]}{3.6 \times 10^6} \\ &+ \frac{\left[\left(750.9 + 115.4 \times n/60 + 11.32 \times (n/60)^2 + 2.256 \times \pi d \cdot n/60 \cdot f \cdot a_p\right) \times t_{cut-1}\right]}{3.6 \times 10^6} \\ &+ \frac{\left[\left(750.9 + 115.4 \times n/60 + 11.32 \times (n/60)^2 + 2.256 \times \pi d \cdot n/60 \cdot f \cdot rem(R-r, a_p)\right) \times t_{cut-2}\right]}{3.6 \times 10^6}, \end{aligned} \tag{18}$$

$$\begin{aligned} t_{idle} &= \frac{498}{19} + ceil\left(\frac{R-r}{a_p}\right) \times \left(\frac{8}{n/60 \cdot f} + \frac{228}{190}\right), \\ t_{cut} &= t_{cut-1} + t_{cut-2}, \\ t_{cut-1} &= floor\left(\frac{R-r}{a_p}\right) \times \frac{30}{n/60 \cdot f}, \\ t_{cut-2} &= ceil\left(rem(R-r, a_p)/\Delta\right) \times \frac{30}{n/60 \cdot f}, \\ T_{tool} &= \frac{60}{f}\left(\frac{6 \times 10^5}{3.1415926 \times n/60}\right)^{2.13}, \end{aligned} \tag{19}$$

where Δ is a corrected coefficient, of which any value greater than the cutting depth will be reasonable.

5 Results and Discussion

5.1 Analysis of Optimization Results

A non-dominated sorting genetic algorithm with an elitist strategy (NSGA-II) is one of the most popular multi-objective genetic algorithms, which reduces the complexity of the non-inferior sorting genetic algorithm and has the advantages of a fast running speed and good convergence of the solution set [30]. In this paper, NSGA-II is employed as a computing tool for the Pareto frontier in multi-objective optimization. The population size is 50 and the reproductive algebra is set to 2000, with the remaining parameters set by default. Matlab R2014a is used to simulate the optimization model, and the Pareto front of the multi-objective optimization is as shown in Figure 5. The corresponding Pareto frontier is shown in Appendix C.

The curve in Figure 5(a) reflects the trade-off among the three objectives. Meanwhile, the relationships between the two targets among the three goals are shown in Figure 5(b), (c), and (d). From Figure 5(b), there is an approximate linear relationship between the processing time and carbon emissions. That is, within the boundary of the system, the increase in the processing time will cause an approximately linear increase in carbon emissions, which has a certain relationship with the selection of the system boundaries, but little effect on the law. From Figure 5(c), the amount of carbon emissions and surface roughness are inversely proportional. This means that reducing the surface roughness often results in greater carbon emissions. The same relationship is also shown between the surface roughness and the processing time (Figure 5(d)).

The cutting parameters for minimizing the carbon emissions are $a_p = 1.5$ mm, $n = 300$ r/min, and $f = 0.3$ mm/r, with 55.57 g of carbon emissions, a processing time of 79.28 s, and a surface roughness of 18.49 μm. The parameters minimizing the processing time are $a_p = 1.5$ mm, $n = 600$ r/min, and $f = 0.3$ mm/r, with carbon emissions of 83.07 g, a processing time of 53.94 s, and a surface roughness of 18.49 μm. Usually, the bigger the cutting parameters are, the smaller the processing time; however, the cutting depth here is not the maximum in the optional interval because the processing task-based optimization model was chosen in this study. When the specified total processing depth is 3 mm, for the maximum spindle speed and feed rate, the total processing time of the cutting depth in the interval [1.5, 2.0] is the same, which is the least used. Here $a_p = 1.5$ mm is given by the Pareto algorithm when considering the other two objectives. Because the surface roughness calculation formula used in this paper is based on geometric formulas, the surface roughness may be the same under different cutting parameters. It is easy to see from the above data that there are no appropriate decision variables to achieve the minimum of the three goals concurrently.

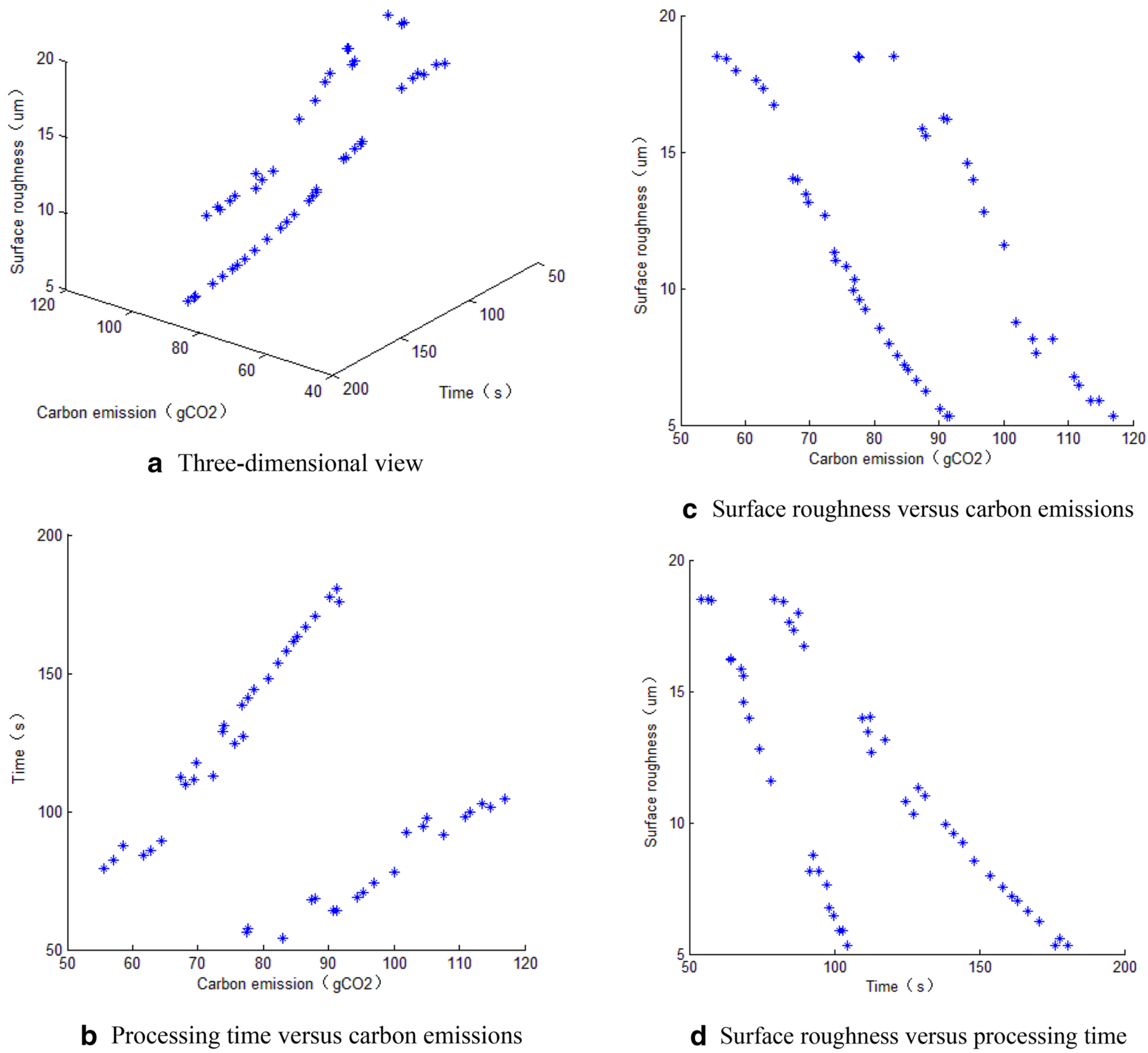

Figure 5 Pareto front of multi-objective optimization

When one of them reaches the minimum, the other two goals are often unsatisfactory.

In general, the Pareto solution set obtained by the multi-objective optimization problem is at the same non-dominated solution level, and there are many solutions with the same degree of congestion, and the dimensions of each optimization target are often different. There is no unified standard, making a comparison difficult, which causes problems for decision makers. Usually, the execution solution is selected from the Pareto frontier based only on subjective consciousness or personal experience. To this end, this study adopts the TOPSIS method to sort the three targets.

In this research, the TOPSIS method is applied to rank the Pareto frontier. TOPSIS is one of the commonly used multi-attribute decision-making methods. The idea is to sort the finite objects to be evaluated based on the ideal optimal and worst values using the Euclidean distance, obtaining the degree of approximation of each point with these values, and thus giving the optimal solution. See Appendix C for the Pareto frontier results. According to the calculation, the optimal approximation is 0.6206, and the corresponding decision variables are $a_p = 1.88$ mm, $n = 560$ r/min, and $f = 0.12$ mm/r. Carbon emissions under the decision variables are 104.94 g·CO_2, the processing time is 97.59 s, and the surface roughness is 7.65 μm.

5.2 Analysis of the Main Effect Factors

To analyze the impact of the decision variables on each goal, the response values of the carbon emissions and processing time are calculated according to Table 4, and an S/N ratio analysis is carried out. The S/N ratio is utilized to measure how the response changes relative to the nominal/target values. For static designs, Minitab offers four signal-to-noise ratios. The purpose of multi-objective optimization in this study is to minimize the carbon emissions, processing time, and surface roughness. Thus, the lower-the-better type of objective function was selected [31]. The conversion relation between the S/N ratio and the signal is as follows:

$$S/N = -10 \times \lg\left(\frac{1}{n}\sum_{i=1}^{n} y_i^2\right), \tag{20}$$

where n is the number of experiments, and y_i is the value of the carbon emissions or processing time.

The S/N ratio at each level for the various factors of the carbon emissions and processing times is plotted in Figures 6 and 7 respectively. As shown in Figure 6, on the whole, the larger the cutting parameters are, the smaller the processing time. The condition at $a_p = 1.5$ mm or 2.0 mm, $n = 600$ r/min, and $f = 0.25$ mm/r can be considered as the level at which the processing time is minimal within the given range of parameters. This is because this study adopted a task-based optimization model, under which the spindle speed and feed rate are fixed, and for a cutting depth of 3 mm, when $a_p = 1.5$ mm or 2.0 mm, two cutting processes are needed, and therefore the processing times under these two sets of cutting parameters are the same. In fact, the machining processing time is the same when the cutting depth is located within the interval [1.5 mm, 2 mm).

In addition, the carbon emissions will be at minimum when $a_p = 2.0$ mm, $n = 300$ r/min, and $f = 0.25$ mm/r within the given range of parameters. From the results, it can be found that, within the selected cutting parameters, the cutting parameters that minimize the carbon emissions differ from those that minimize the processing time, even the law of change is reversed (the spindle speed has the opposite effect on the carbon emissions and processing time). However, whether it is for the carbon emissions or processing time, the optimal result depends on the selected cutting parameters. The selection of the cutting parameter values directly determines the accuracy of the optimization results. This means that the optimal values of this part are only optimal among the selected discrete cutting parameters and are not globally optimal.

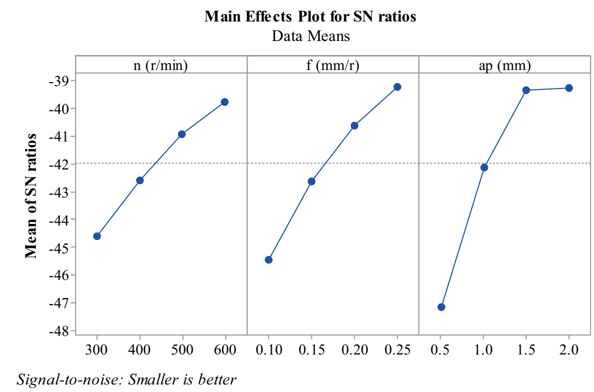

Figure 6 Main effects plot for processing time

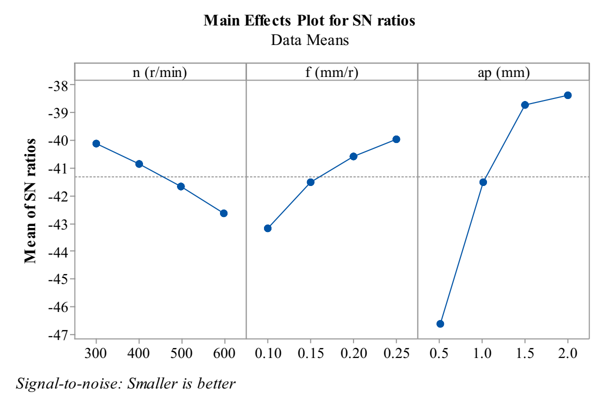

Figure 7 Main effects plot for carbon emissions

Table 4 Levels and factors selected for S/N ratios

	Spindle speed (r/min)	Feed rate (mm/r)	Cutting depth (mm)
1	300	0.1	0.5
2	400	0.15	1
3	500	0.2	1.5
4	600	0.25	2

Tables 5 and 6 are the S/N ratios of the carbon emissions and processing time, respectively. A first rank contribution is assigned to the highest range value. For both the carbon emissions and processing time, the cutting depth is the most significant factor, followed by the feed rate, and the spindle speed is the least significant factor.

5.3 Coupling Effect Analysis

The effect of the cutting parameters on the carbon emissions and processing time based on the processing task in this study can be observed from the contour plots in

Table 5 S/N ratios of carbon emissions

Level	a_p	n	f
1	− 46.62	− 40.11	− 43.16
2	− 41.52	− 40.83	− 41.51
3	− 38.72	− 41.66	− 40.58
4	− 38.37	− 42.63	− 39.97
Delta	8.25	2.52	3.19
Rank	1	3	2

Table 6 S/N ratios of processing time

Level	a_p	n	f
1	− 47.17	− 44.6	− 45.45
2	− 42.14	− 42.62	− 42.64
3	− 39.34	− 40.94	− 40.61
4	− 39.27	− 39.76	− 39.22
Delta	7.89	4.84	6.23
Rank	1	3	2

Figures 8 and 9. For the processing time during the turning process, in general, the greater the values of the cutting parameters are, the shorter the processing time, although the influence rate of the decision variables on the processing time is different. The effect of the cutting depth on the processing time is more significant than that of the spindle speed on the processing time based on the contour map (Figure 8(a)). The effect of the cutting depth on the processing time is more significant than that of the feed rate on the processing time (Figure 8(b)). The effect of the feed rate on the processing time is more significant than that of the spindle speed (Figure 8(c)). The influence of the cutting depth, feed rate, and spindle speed on the processing time is gradually weakened. This is consistent with the analysis results in Section 5.2. Thus, the minimum processing time can be achieved when the levels of the spindle speed, feed rate, and cutting depth are at their highest levels.

The value of the carbon emissions is minimized when the cutting depth and the feed rate were at their highest values, and the spindle speed was at its lowest value (Figure 9). Moreover, as stated in the graphs, the effects

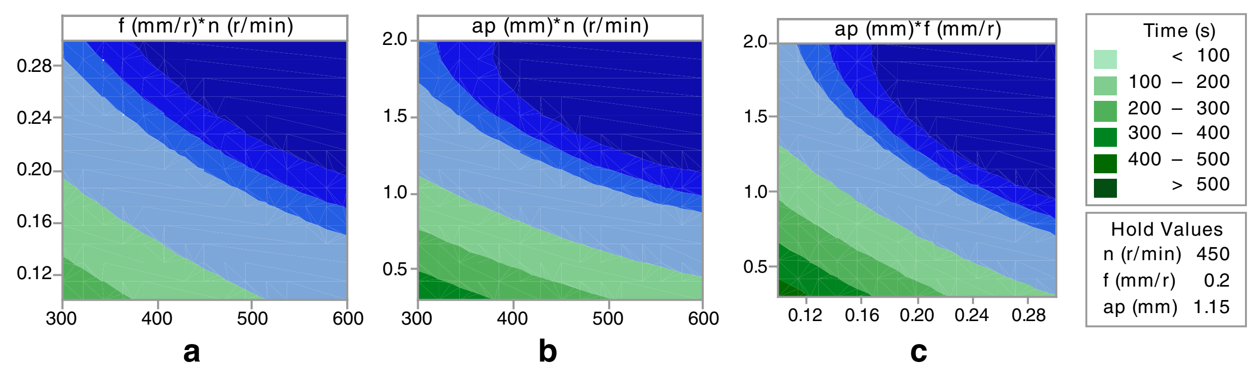

Figure 8 Contour plots of processing time

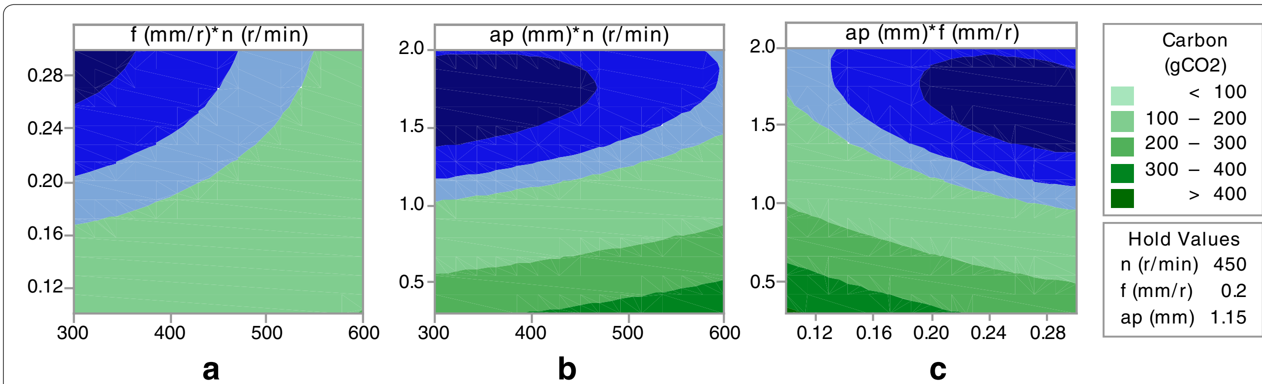

Figure 9 Contour plots of carbon emission

of the cutting depth on the carbon emissions are more significant than those of the spindle speed on the carbon emission (Figure 9(a)), whereas the effects of the cutting depth on the carbon emissions are more significant than the feed rate on the carbon emissions (Figure 9(b)), This is also consistent with the analysis results in Section 5.2.

5.4 Sensitivity Analysis

To further analyze the changing rules of the target to be evaluated with the decision variables, a sensitivity analysis method is adopted (Figures 10, 11, 12). From the perspective of the target to be evaluated, it is easy to find that the processing time decreases monotonously with the increase in the three decision variables. The carbon emissions decreased monotonously with an increase in the feed rate and the cutting depth; however, with an increase in the spindle speed, the carbon emissions show a decreasing trend first, followed by an increasing trend. From the impact of the decision variables on the evaluation objectives, the objectives to be optimized vary smoothly with the spindle speed and feed rate, but with an increase in the cutting depth, they show a stepped decrease. This is because, in this study, a processing task-based optimization model was selected, and for the processing depth (3 mm) specified in this paper, a cutting depth that can be divided by 3 without any remainder (e.g., 0.5 mm, 0.75 mm, 1.0 mm, 1.5 mm) is a watershed for the processing time and carbon emissions. Between the two watersheds, although the cutting depth changes, the total processing time remains unchanged. However, the processing time at the watershed will decline in a cliff-like descent. This is because, at the watershed, the cutting cycle processing times will change suddenly, which will lead to the step change in the processing time. The step change of the processing time directly affects the step change of the carbon emissions. However, there is a weak upward trend in carbon emissions between the two watersheds, the reason for which is as follows: although the processing times between the two watersheds are constant, that is, the idle time and cutting time remain unchanged, with the increase in the cutting depth, the deviation between the setting of the cutting depth and the cutting depth during the last cutting increases, which causes an increase in the cutting power fluctuation of the machine tool, leading to an increase in the energy consumption during the entire processing process, naturally causing an increase in the carbon emissions.

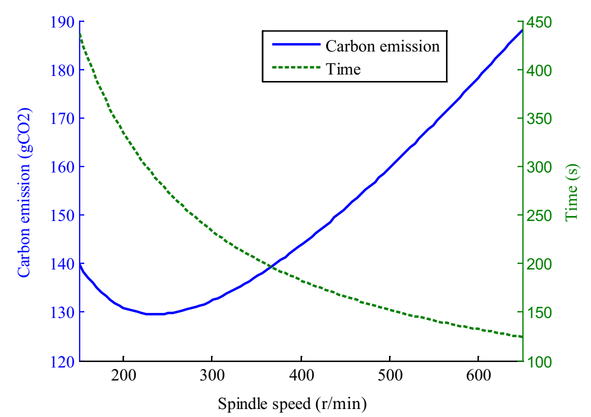

Figure 10 Influence of spindle speed on the optimization target

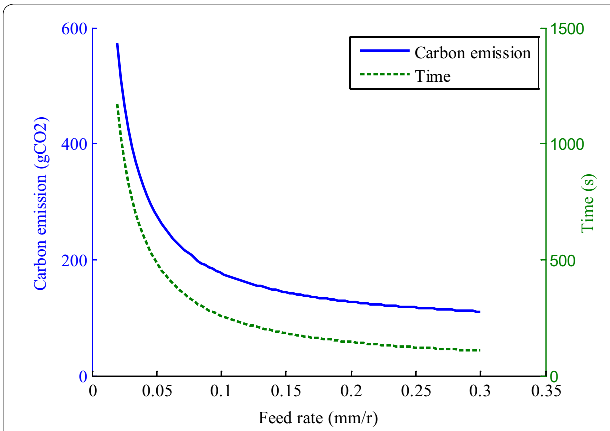

Figure 11 Influence of feed rate on the optimization target

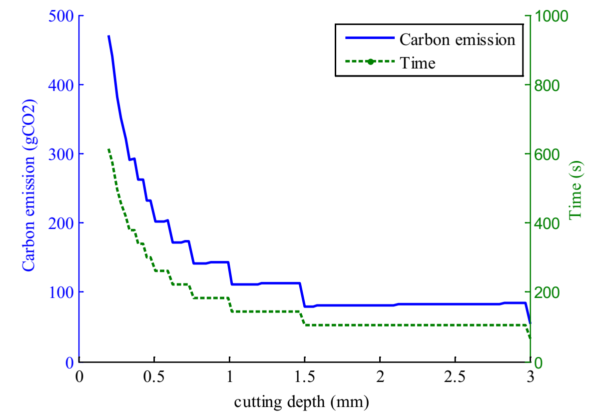

Figure 12 Influence of cutting depth on the optimization target

6 Conclusions

In this study, a task-based multi-objective optimization model that incorporates the environment impact, product quality, and processing efficiency was considered, and the following conclusions were obtained.

1. Different optimal cutting parameters were obtained for different optimization purposes. When only the processing time is optimized, the cutting parameters

selected should be as large as possible. When only the surface roughness is optimized, a smaller feed rate should be selected. When only carbon emissions are optimized, the cutting parameters need to be considered comprehensively, as is the case when the three targets are simultaneously optimized.

2. The cutting depth among the other parameters has the most significant effect on both the carbon emissions and processing time, and the spindle speed has the least significant effect by comparison, with the feed rate being between them.
3. The variation of the carbon emissions and processing time with the decision variables is analyzed. The reason for the decrease in carbon emissions and time in a cliff-like descent is analyzed emphatically. This also explains the reason for the slight increase in carbon emissions between the two watersheds.
4. Future studies will be conducted on milling, grinding, drilling, and other extensions. Meanwhile, factors such as the cutting tools and machining operations will be added to the decision variables, and the decision variables will be optimized to find the trade-off that takes the environment impact, product quality, processing efficiency, and even cost into account.

Abbreviations

A: a constant denoting the coefficient related to the operation conditions; a_p: the depth of the cut (mm); *C*: total carbon emissions in metal cutting processes (g); C_{consum}: consumable carbon emissions (g); C_{air}: carbon emissions for preparing compressed air (g); C_{chips}: carbon emissions from chips (g); C_{cool}: carbon emissions from the use of coolant (g); $C_{cool\text{-}w}$: carbon emissions from waste coolant (g); $CF_{c\text{-}pro}$: carbon emission factor of coolant fluid production (g-CO_2/L); $CF_{c\text{-}dis}$: carbon emission factor for waste coolant disposal (g-CO_2/L); $CF_{disposal}$: carbon emission factor for chips disposal (g-CO_2/kg); CF_{ene}: carbon emission factor of electricity (g/kwh); $CF_{material}$: carbon emission factor of material production (g-CO_2/kg); CF_{tool}: carbon emission factor of cutting tools (g-CO_2/g); $C_{resource}$: carbon emission caused by resource depletion (g); C_{trans}: transferable (transitional) carbon emissions (g); C_{tool}: carbon emissions caused by tools, which include tool usage stage and tool sharpening process (g); $C_{tool\text{-}w}$: carbon emissions from scrap tool treatment (g); C_{waste}: carbon emissions caused by waste generation (g); E_{ene}: energy consumption of machine tools (kW·h); *f*: feed rate (mm/r); *h*: spindle speed, feed rate, and depth of cut; M_{tool}: weight of a tool (g); *n*: spindle speed (r/min); R_a: roughness height; *t*: the sum of t_{idle} and t_{cut}(s); t_{chan}: tool changing processing time (s); t_{cut}: the actual cutting processing time (s); t_{clam}: Workpiece clamping processing time (s); $t_{stand\text{-}by}$: the period when the machine tool stays without any operations (s); t_{idle}: the period when the spindle rotates without cutting (s); t_{set}: tool setting processing time (s); t_{pro}: programming time (ignored during mass processing) (s); t_{unl}: unloading blank processing time (s); T_{tool}: life cycle of cutting tools (min); *x*, *y*, *z*, *m*: influence index; *β*: the coefficients of each term; *ε*: residual error.

Authors' Contributions

YL and DG were in charge of the whole trial; ZJ wrote the manuscript; XL assisted with sampling and laboratory analyses. All authors read and approved the final manuscript.

Authors' Information

Zhipeng Jiang, born in 1988, is currently a PhD candidate at *Harbin Institute of Technology, China*. His research interests include green manufacturing and mechatronics engineering.

Dong Gao, born in 1970, is currently an professor at *Harbin Institute of Technology, China*. He received his PhD degree from *Harbin Institute of Technology, China*, in 1999. His research interests include sustainable manufacturing techniques and error modeling and compensation for heavy-duty machine tool.

Yong Lu, born in 1971, is currently an professor at *Harbin Institute of Technology, China*. He received his PhD degree from *Harbin Institute of Technology, China*, in 2000. His research interests include space on-orbit service technology and intelligent tool condition monitoring technology.

Xianli Liu, born in 1961, is currently an professor at *Harbin University of Science & Technology, China*. His research interests include high efficiency machining and cutting tool technology.

Competing interests

The authors declare that they have no competing interests.

Funding

Supported by National Hi-tech Research and Development Program of China (863 Program, Grant No. 2014AA041503), and National Natural Science Foundation of China (Key Program, Grant No. 51235003).

Author Details

[1] School of Mechatronics Engineering, Harbin Institute of Technology, Harbin 150001, China. [2] State Engineering Laboratory of High Efficiency Cutting and Tool, Harbin University of Science and Technology, Harbin 150080, China.

Appendix A. Response Surface Analysis

Minitab was used to analyze the response surface experiment, and a variance analysis, model summary, and regression model of the surface roughness were obtained.

The regression equation in uncoded units space is as follows:

$$\begin{aligned} Ra = &-10.99 + 0.0049V_c + 194f + 0.95a_p \\ &- 0.000015V_c^2 - 321.5f^2 - 0.485a_p^2 \\ &- 0.0357V_cf - 0.00361V_ca_p + 3.24fa_p. \end{aligned} \tag{21}$$

1. Considering the total effect in Table 7, in this case, the P value of the regression term is 0.000, which indicates that the original hypothesis should be rejected and that the model is generally valid. Meanwhile, the P value of a lack-of-fit is 0.203, which is significantly higher than the significant level of 0.05. Accepting the original hypothesis, it is considered that there is no unfit phenomenon in this model.
2. Considering the total effect of the fit, in this case, R-Sq is close to R-Sq(adj), and the fitting effect of the model is considered good. Here, R-Sq (pred) is closer to the R-Sq value, which is larger, indicating that the future prediction using this model is reliable (Table 8).
3. Considering the significance of each effect, it can be seen from the table that the corresponding probability values of feed rate f and its squared term are less than 0.05, indicating that these effects are significant. The probability values corresponding to the other items are far greater than 0.05, which is obviously greater than the significant level. It is considered that these items are not significant.

Table 7 Analysis of variance

Source	DF	Adj SS	Adj MS	F-Value	P-Value
Model	9	493.989	54.8877	216.03	0.000
Linear	3	1.798	0.5992	2.36	0.133
Vc	1	0.002	0.0021	0.01	0.929
f	1	1.737	1.7370	6.84	0.026
ap	1	0.059	0.0585	0.23	0.642
Square	3	59.374	19.7914	77.90	0.000
Vc*Vc	1	0.001	0.0006	0.00	0.961
f*f	1	28.426	28.4262	111.88	0.000
ap*ap	1	0.337	0.3371	1.33	0.276
2-way interaction	3	0.781	0.2604	1.02	0.422
Vc*f	1	0.100	0.0999	0.39	0.545
Vc*ap	1	0.074	0.0741	0.29	0.601
f*ap	1	0.607	0.6072	2.39	0.153
Error	10	2.541	0.2541		
Lack-of-fit	5	1.747	0.3494	2.20	0.203
Pure error	5	0.794	0.1587		
Total	19	496.530			

Table 8 Model summary

S	R-sq (%)	R-sq (adj) (%)	R-sq (pred) (%)
0.504053	99.49	99.03	97.21

Based on the above analysis, we know that, except for feed rate f and its squared term, the other items are not significant and should be eliminated, and thus we need to re-fit the new model.

Regression equation in uncoded units,

$$Ra = -11.556 + 203.16f - 343.4f^2. \tag{22}$$

1. The P value of the regression term is 0.000 (Table 9), which indicates that the original hypothesis should be rejected and that the model is generally valid. Meanwhile, the P value of a lack-of-fit is 0.219, which is significantly higher than the significant level of 0.05. Accepting the original hypothesis, it is considered that there is no unfit phenomenon even though seven items are deleted from the model.
2. Although there are seven fewer items in the model, R-Sq is close to R-Sq(adj), and the fitting effect of the model is considered good. R-Sq (pred) is closer to the R-Sq value, which is larger, indicating that the future prediction using this model is reliable (Table 10).

Table 9 Analysis of variance

Source	DF	Adj SS	Adj MS	F-Value	P-Value
Model	2	491.814	245.907	886.47	0.000
Linear	1	432.846	432.846	1560.36	0.000
f	1	432.846	432.846	1560.36	0.000
Square	1	58.969	58.969	212.58	0.000
f*f	1	58.969	58.969	212.58	0.000
Error	17	4.716	0.277		
Lack-of-fit	12	3.922	0.327	2.06	0.219
Pure error	5	0.794	0.159		
Total	19	496.530			

Table 10 Model summary

S	R-sq (%)	R-sq (adj) (%)	R-sq (pred) (%)
0.526689	99.05	98.94	98.65

3. It can be seen from the table that the corresponding probability values of feed rate f and its squared term are less than 0.05, indicating that these two effects are significant. This shows that the effect of the regression is still good after deleting the insignificant interaction.

Appendix B. Processing Time Calculation

As the requirement of the experiment mentioned above, a bar with a diameter of 90 mm is required to be machined to a diameter of 84 mm, that is, the total cutting depth on one side is 3.0 mm. When the cutting depth is set at 0.5, 1.0, 1.5, and 2.0 mm, the cycle is six, three, two, and two processing times, respectively. For a 2.0 mm cutting depth, two cycles are needed, one for a cutting depth of 2.0 mm, and the other for a cutting depth of 1.0 mm instead of 2.0 mm. Then, the fourth set of experimental parameters in Table 3 were taken as an example calculation.

During the experiment, the tool path (fast forward, feed, and withdraw) and the distance were as shown in Figure 2, with $L_{x1} = 200$, $L_{z1} = 400$, $L_{z2} = 2$, $L_{z3} = 30$, and $L_{x2} = 6$. The standby processing time of each group is set at a fixed value of 30 s, and combined with the information of the machine tool coordinate system settings, the idle running processing time will be as follows:

$$
\begin{aligned}
t_{idle} &= \frac{400}{1900/60} + ceil\left(\frac{3}{a_p}\right) \\
&\quad \times \left(\frac{8}{n/60 \cdot f} + \frac{38}{1900/60}\right) + \frac{430}{1900/60} \\
&= \frac{498}{19} + ceil\left(\frac{3}{a_p}\right) \times \left(\frac{480}{n \cdot f} + \frac{228}{190}\right).
\end{aligned} \tag{23}
$$

Although the cutting depth is set to a certain value, the total depth to be cut is not necessarily an integral multiple of the cutting depth. When the cutting depth is different from the set cutting depth in the last cutting, the cutting power of the machine tool will change. Therefore, this study calculated the processing time with the same cutting depth as the set cutting depth, and the processing time with a different cutting depth as the set cutting depth, which were called t_{cut-1} and t_{cut-2}, respectively. When the total depth to be machined is an integer multiple of the set cutting depth, $t_{cut-2} = 0$.

$$
\begin{aligned}
t_{cut} &= t_{cut-1} + t_{cut-2}, \\
t_{cut-1} &= floor\left(\frac{R-r}{a_p}\right) \times \frac{30}{n/60 \cdot f}, \\
t_{cut-2} &= ceil\left(rem\left(R-r, a_p\right)/\Delta\right) \times \frac{30}{n/60 \cdot f}.
\end{aligned} \tag{24}
$$

Appendix C. Carbon Emission Calculation

Carbon Emissions from Consumable Carbon Emissions

Combined with the power calculation formula of the machine tools, the carbon emissions from the consumable carbon emissions is as follows:

$$
\begin{aligned}
E_{ene} &= \frac{\left[321.4 \times 30 + \left(750.9 + 115.4 \times n/60 + 11.32 \times (n/60)^2\right) \times t_{idle}\right]}{3.6 \times 10^6} \\
&\quad + \frac{\left[\left(750.9 + 115.4 \times n/60 + 11.32 \times (n/60)^2 + 2.256 \times \pi d \cdot n/60 \cdot f \cdot a_p\right) \times t_{cut-1}\right]}{3.6 \times 10^6} \\
&\quad + \frac{\left[\left(750.9 + 115.4 \times n/60 + 11.32 \times (n/60)^2 + 2.256 \times \pi d \cdot n/60 \cdot f \cdot rem\left(R-r, a_p\right)\right) \times t_{cut-2}\right]}{3.6 \times 10^6},
\end{aligned} \tag{25}
$$

$$
C_{consum} = 724.2 \times E_{ene}. \tag{26}
$$

Carbon Emissions from Cutting Tools

The carbon emissions from the cutting tools includes carbon emissions from the tool production and from tool re-sharpening after a tool failure. The tool re-sharpening process is not included in this case owing to limited conditions. The tool quality is 474 g, and therefore, the carbon emissions caused by tool wear can be obtained.

$$
C_{tool} = \frac{t_{cut}}{T_{tool}} \times 29.6 \times 474. \tag{27}
$$

The calculating method of the tool life is shown in the following formula. According to the cutting parameters, the calculating method of the tool life is obtained [25]:

$$
T_{tool} = \frac{60}{f}\left(\frac{6 \times 10^5}{3.1415926 \times n/60}\right)^{2.13}. \tag{28}
$$

Carbon Emissions from Coolant Fluid

Thus, carbon emissions caused by coolant can be calculated based on Section 4.1.

$$
\begin{aligned}
C_{cool} &= \frac{(t_{cut} + t_{idle})}{5 \times 22 \times 8 \times 60 \times 60}(2850 \times 20 + 4000 \times 8) \\
&= \frac{(t_{cut} + t_{idle})}{3168} \times 89.
\end{aligned} \tag{29}
$$

Thus, the formula for calculating the carbon emissions is as follows:

$$
C = 724.2 \times E_{ene} + \frac{t_{cut}}{T_{tool}} \times 14030.4 + \frac{(t_{cut} + t_{idle})}{3168} \times 89. \tag{30}
$$

Appendix D. Pareto Front Solution Set

Table 11 shows the corresponding Pareto frontier of the multi-objective optimization in this study. In addition, the cutting parameters corresponding to the lowest target are marked.

Table 11 Pareto front solution set

No.	Cutting depth (mm)	Spindle speed (r/min)	Feed rate (mm)	Carbon emissions (g-CO_2)	Processing time (s)	Surface roughness (μm)	Relative closeness	Note
1	1.50	300	0.30	55.57	79.28	18.49	0.5007	Minimum carbon emission
2	1.50	300	0.10	91.26	180.61	5.33	0.4943	Minimum surface roughness
3	1.50	300	0.10	91.26	180.61	5.33	0.4943	Minimum surface roughness
4	1.50	600	0.30	83.07	53.94	18.49	0.5029	Minimum processing time
5	1.93	600	0.10	116.97	104.61	5.33	0.6056	Minimum surface roughness
6	1.51	546	0.30	77.39	56.48	18.49	0.5073	
7	1.99	600	0.19	94.31	68.83	14.57	0.5378	
8	1.66	335	0.22	64.48	89.43	16.70	0.5000	
9	1.52	300	0.13	78.50	144.21	9.22	0.5175	
10	1.53	300	0.26	58.61	87.56	17.99	0.4885	
11	1.53	333	0.25	61.72	84.31	17.64	0.4965	
12	1.89	560	0.13	101.99	92.52	8.76	0.6187	
13	1.53	336	0.24	62.74	85.92	17.31	0.4979	
14	1.55	300	0.15	74.01	131.14	11.02	0.5172	
15	1.52	326	0.15	75.68	124.45	10.80	0.5407	
16	1.98	559	0.20	87.94	68.55	15.61	0.5259	
17	1.61	300	0.28	57.08	82.42	18.43	0.4934	
18	1.54	300	0.11	86.51	166.75	6.64	0.5042	
19	1.52	300	0.12	83.44	158.22	7.55	0.5102	
20	1.57	310	0.18	68.07	109.66	13.99	0.5093	
21	1.50	300	0.10	90.22	177.63	5.59	0.4966	
22	1.55	300	0.18	67.41	112.31	14.01	0.5026	
23	1.55	301	0.14	76.72	138.38	9.94	0.5193	
24	1.53	300	0.11	87.92	170.81	6.24	0.5012	
25	1.89	590	0.11	110.87	98.26	6.77	0.6162	
26	1.59	314	0.17	69.44	111.70	13.46	0.5154	
27	1.94	599	0.10	114.82	101.59	5.91	0.6102	
28	1.88	560	0.12	104.94	97.59	7.65	0.6206	Minimum overall
29	1.51	309	0.10	91.55	176.00	5.33	0.5021	Minimum surface roughness
30	1.91	567	0.12	104.45	94.49	8.13	0.6199	
31	1.52	300	0.11	84.60	161.31	7.19	0.5084	
32	1.98	594	0.12	107.61	91.45	8.14	0.6165	
33	1.55	301	0.13	77.70	141.14	9.57	0.5189	
34	1.95	600	0.21	91.19	64.18	16.18	0.5153	
35	1.77	600	0.17	96.91	74.07	12.81	0.5677	
36	1.98	596	0.21	90.75	64.28	16.22	0.5150	
37	1.72	300	0.17	69.77	117.41	13.16	0.5063	
38	1.51	300	0.11	85.11	163.05	7.02	0.5071	
39	1.71	327	0.17	72.28	112.90	12.66	0.5288	
40	1.95	600	0.15	100.03	78.02	11.57	0.5851	
41	1.50	544	0.29	77.71	57.56	18.48	0.5051	
42	1.96	558	0.21	87.39	67.91	15.83	0.5231	
43	1.92	600	0.10	116.92	104.61	5.33	0.6057	Minimum surface roughness
44	2.00	599	0.18	95.29	70.59	13.99	0.5469	
45	1.55	301	0.12	82.24	153.67	7.99	0.5140	
46	1.89	589	0.11	111.72	99.91	6.46	0.6149	
47	1.54	304	0.13	80.70	148.25	8.52	0.5190	
48	1.71	300	0.15	73.85	129.08	11.32	0.5150	

Table 11 (continued)

No.	Cutting depth (mm)	Spindle speed (r/min)	Feed rate (mm)	Carbon emissions (g-CO_2)	Processing time (s)	Surface roughness (μm)	Relative closeness	Note
49	1.52	327	0.14	76.88	127.17	10.33	0.5428	
50	1.92	587	0.10	113.51	103.03	5.90	0.6110	

Received: 26 March 2019 Revised: 10 July 2019 Accepted: 4 November 2019
Published online: 27 November 2019

References

[1] Ministry of Ecology and Environment of the People's Republic of China. China Vehicle Environmental Management Annual Report (2018). http://www.vecc-mep.org.cn/huanbao/content/944.html. (in Chinese)
[2] X L Liu, Z P Jiang, M Y LI, et al. New rounded end mill for mold processing based on scallop-height. *Journal of Mechanical Engineering*, 2015, 51(5): 192-204. (in Chinese)
[3] D F Liu, X J Zhang. The influence of hard turning technology on product quality and cost. *Die and Mould Technology*, 2006, 5(6): 57-60. (in Chinese)
[4] https://unfccc.int/process-and-meetings/the-kyoto-protocol/what-is-the-kyoto-protocol/what-is-the-kyoto-protocol /(accessed on 24 May 2019).
[5] R Huang, M Riddle, D Graziano, et al. Energy and emissions saving potential of additive manufacturing: The case of lightweight aircraft components. *Journal of Cleaner Production*, 2016, 135: 1559-1570.
[6] R Li, Q Zhang, X Zhang, et al. Control method for steel strip roughness in Two-stand temper mill rolling. *Chinese Journal of Mechanical Engineering*, 2015, 28(3): 573-579.
[7] D B Tang, M Dai. Energy-efficient approach to minimizing the energy consumption in an extended job-shop scheduling problem. *Chinese Journal of Mechanical Engineering*, 2015, 28(5): 1048-1055.
[8] G Campatelli, L Lorenzini, A Scippa. Optimization of process parameters using a Response Surface Method for minimizing power consumption in the milling of carbon steel. *Journal of Cleaner Production*, 2014, 66(2): 309-316.
[9] J Wójcicki, M Leonesio, G Bianchi, et al. Integrated energy analysis of cutting process and spindle subsystem in a turning machine. *Journal of Cleaner Production*, 2018, 170: 1459-1472.
[10] Q Zhong, R Tang, T Peng. Decision rules for energy consumption minimization during material removal process in turning. *Journal of Cleaner Production*, 2016, 140: 1819-1827.
[11] P S Bilga, S Singh, R Kumar. Optimization of energy consumption response parameters for turning operation using Taguchi method. *Journal of Cleaner Production*, 2016, 137: 1406-1417.
[12] B Wang, Z Liu, Q Song, et al. Proper selection of cutting parameters and cutting tool angle to lower the specific cutting energy during high speed machining of 7050-T7451 aluminum alloy. *Journal of Cleaner Production*, 2016, 129: 292-304.
[13] Q Wang, F Liu, X Wang. Multi-objective optimization of cutting parameters considering energy consumption. *International Journal of Advanced Manufacturing Technology*, 2014, 71(5-8): 1133-1142.
[14] Q Yi, C Li, Y Tang, et al. Multi-objective parameter optimization of CNC machining for low carbon manufacturing. *Journal of Cleaner Production*, 2015, 95: 256-264.
[15] Z J Liu, D P Sun, C X Lin, et al. Multi-objective optimization of the operating conditions in a cutting process based on low carbon emission processing times. *Journal of Cleaner Production*, 2016, 124: 266-275.
[16] K He, R Tang, M Jin. Pareto fronts of cutting parameters for trade-off among energy consumption, cutting force and processing time. *International Journal of Production Economics*, 2017, 185: 113-127.
[17] S A Bagaber, A R Yusoff. Multi-objective optimization of cutting parameters to minimize power consumption in dry turning of stainless steel 316. *Journal of Cleaner Production*, 2017, 157: 30-46.
[18] W W Lin, D Y Yu, et al. Multi-objective teaching–learning-based optimization algorithm for reducing carbon emission and operation processing time in turning operations. *Engineering Optimization*, 2015, 47(7): 994-1007.
[19] C Camposeco-Negrete. Optimization of cutting parameters using Response Surface Method for minimizing energy consumption and maximizing cutting quality in turning of AISI 6061 T6 aluminum. *Journal of Cleaner Production*, 2015, 91: 109-117.
[20] W W Lin, D Y Yu, C Y Zhang, et al. Multi-objective optimization of machining parameters in multi-pass turning operations for low-carbon manufacturing. *Proceedings of the Institution of Mechanical Engineers Part B Journal of Engineering Manufacture*, 2017, 231(13): 2372-2383.
[21] Ic Yusuf Tansel, Saraloğlu Güler Ebru, Cabbaroğlu Ceren, et al. Optimisation of cutting parameters for minimizing carbon emission and maximising cutting quality in turning process. *International Journal of Production Research*, 2018, 56(11): 1-21.
[22] C Li, Q Xiao, Y Tang, et al. A method integrating Taguchi, RSM and MOPSO to CNC cutting parameters optimization for energy saving. *Journal of Cleaner Production*, 2016, 135: 263-275.
[23] Y Zhang, Q Liu, Y Zhou. Integrated optimization of cutting parameters and scheduling for reducing carbon emission. *Journal of Cleaner Production*, 2017, 53(5): 886-895.
[24] F Ma, H Zhang, H J Cao, Multi-objective cutting parameters optimization for low energy and minimum cutting fluid consumption. *Journal of Mechanical Engineering*, 2017, 53(11): 157-163. (in Chinese)
[25] C B Li . Multi-objective NC cutting parameters optimization model for high efficiency and low carbon. *Journal of Mechanical Engineering*, 2013, 49(9): 87-96. (in Chinese)
[26] Z P Jiang, D Gao, Y Lu, et al. Electrical energy consumption of CNC machine tools based on empirical modeling. *The International Journal of Advanced Manufacturing Technology*, 2018, https://doi.org/10.1007/s00170-018-2808-x.
[27] Z H Zhou. *Metal cutting theory*. Shanghai Scientific and Technical Publishers, 1984. (in Chinese)
[28] S Kalpakjian, S R Schmid. *Manufacturing engineering and technology: machining*. Beijing: China Machine Press, 2006.
[29] E Oberg, F D Jones, H L Horton. *Machinery's Handbook*. 26th ed. New York: Industrial Press Inc., 2000.
[30] K Deb, A Pratap, S Agarwal, et al. A fast and elitist multiobjective genetic algorithm: NSGA-II. *IEEE Transactions on Evolutionary Computation*, 2002, 6(2): 182-197.
[31] G Box. Signal-to-noise ratios, performance criteria, and transformations. *Technometrics*, 1988, 30(1): 1-17.